Copyright © 1996 Elsevier Science Ltd
Paper No. 366. (quote when citing this article)
Eleventh World Conference on Earthquake Engineering
ISBN: 0 08 042822 3

LIQUEFACTION HAZARD MAPPING OF REGIONAL AREA BY USING GEOGRAPHIC INFORMATION SYSTEM

T.KOIKE, T.IMAI and T.KANEKO

Kawasaki Steel Corporation, Steel Structure Laboratories
351 Naganuma-cho, Inage-ku, Chiba 263 JAPAN

ABSTRACT

A new methodology to predict the liquefaction hazard of the regional area is proposed. This method can be incorporated in GIS to develop regional liquefaction hazard maps which are needed for routing of major lifelines and siting of major facilities. A quantitative liquefaction hazard for a geomorphological land classification map in terms of the occurrence is built up by using the Digital National Land Information and the location data of liquefaction in the historic earthquakes in Japan. Prediction for the 1987 Chibaken-toho-oki earthquake was conducted based on the results of the analysis for several major historic earthquakes in Kanto district in Japan and shows the good agreement with observations of liquefaction in that earthquake.

KEYWORDS

Liquefaction hazard; mapping; GIS; probability; digital national land information; geomorphological land classifications; microzonation

INTRODUCTION

There are several methods (Matsuoka, Midorikawa and Wakamatsu, 1993) currently used to evaluate the liquefaction hazard, and they vary from generally qualitative to highly quantitative methods. Current qualitative methods include geologic descriptions of deposits, gradation of the soil stratum and depth to groundwater together with topographical informationsof delta, reclaimed land, sand dune, alluvial fan and so on. On the other hand, quantitative methods include a large variety of approaches to evaluate liquefaction with the use of in-situ measurement to evaluate the resistance to liquefaction, the laboratory tests and dynamic analyses. For the practical application of a regional seismic hazard and risk analysis, however, a simple and quantitative method to evaluate hazard is most appropriate especially in the planning and design stages of long-extended pipelines, highways and embankments.

A new methodology to predict the liquefaction hazard of the regional area is proposed in this study. This method can be incorporated in GIS (Geographic Information System, Star and Estes, 1990) to develop regional liquefaction hazard maps which are needed for routing of major lifelines and siting of major facilities.

The microzonation for liquefaction hazard maps is made with the Digital National Land Information (National Land Agency, 1991) which covers the whole area of Japan with 1 km $\times$ 1 km micromeshes, and provides the various kinds of surface geological informations including soil and topographical properties and surface elevations. Current studies point out from the site investigations of liquefaction that the liquefaction-sensitive areas are alluvial delta, reclamaited ground, sandhill and so on. Those geological sites could be classified as geomorphological land. A quantitative estimation of the liquefaction hazard for those geomorphological land classification is built up by using the location data catalog of liquefaction in the historic earthquakes which was furnished by Wakamatsu (1991). Probabilistic approach is adopted herein to take into account the uncertainties in geotechnical and earthquake engineering such as the geological and topographical site conditions, the analytical model used and the magnitude, acceleration and location of the seismic event.

MICROZONING FOR LIQUEFACTION ANALYSIS

Geomorphological land classification

The Digital National Land Information can be utilized to identify each micromesh with its own surface soil type which could be closely related with liquefaction hazard. The twenty different groups of surface soil types including alluvial delta, reclaimed ground, sandhill and so on are selected as the liquefaction-sensitive geomorphological land classifications as shown in Table 1. Each mesh must be given its geological code G_j, (j=1,2,----,20) of Table 1. It should be noted that the geological code 16 to 20 are often assigned to the mesh which locates near the bank of river in the hillsides or mountain areas.

Table 1. Geomorphological land classification.

Stratum	Geomorphological classification	Soil	Geological code
alluvial deposit	delta	gravel	1
		sand	2
		silt	3
		sandy gravel	4
		silty sand	5
		silty sand & gravel	6
	natural levee	heap with mud	7
		heap without mud	8
	sand dune	sand	9
	alluvial fan		10
	others		11
reclaimed land			12
polder			13
beach			14
riverside field			15
diluvial deposit	loam platau		16
	delta		17
	natural leeve		18
	others		19
pre-tertiary deposit			20

Ground motion for microzones

The ground response $S_V(x)$ of the microzone at the site (x) with the geological characteristics G(x) is obtained by multiplying the amplification factor H{G(x)} into the peak ground velocity v(x) on stiff soil as shown in Fig.1. The baserock velocity is obtained from the attenuation relationship for rock motions (Tokimatu and Katayama, 1986). The amplification factor is furnished by Matsuoka and Midorikawa (1993) who derived the regression formula as the function of the site elevation and the shortest distance from a river to estimate the amplification factor for each geological characteristics.

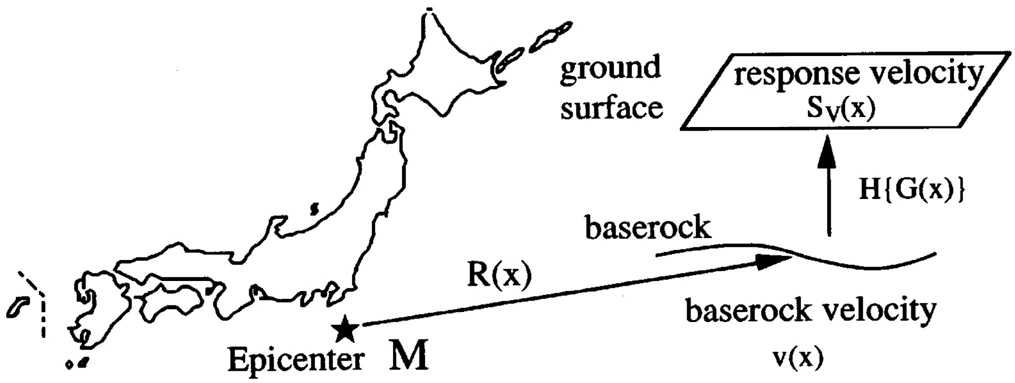

Fig.1 Surface ground response.

LIQUEFACTION ANALYSES

Conditional probablity of liquefaction

The proposed method involves the following five steps:

(1) to assign a regional area, the maximum size of which is approximately 200 km × 200 km;

(2) to collect historical earthquakes in the vicinity of this regional area, the liquefaction sites of which are identified by Wakamatsu (1991).

(3) to calculate the seismic intensity of each mesh converted from the response velocity through the relationship of Fig.2 (Midorikawa and Fukuoka, 1988).

(4) to obtain the liquefaction hazard graph which can be evaluated as the ratio of the number of liquefied meshes against the total number of the meshes with the same geological condition in this regional area; and finally,

(5) to build up the liquefaction hazard maps for the simulated earthquake specifying its magnitude and epicenter.

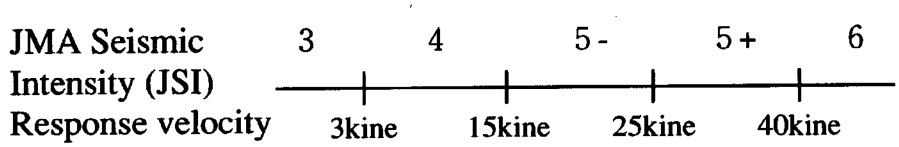

Fig.2 Japan Meteorological Agency seismic intensity (JSI) converted from the response velosity of ground surface (Midorikawa and Fukuoka, Midorikawa and Wakamatsu, 1988).

When the i-th historical earthquake is assigned, the probability of liquefaction under the condition of the seismic intensity k and each geological code G_j is given by

$$P\left[L^i \mid k,G_j\right] = \frac{n^i{}_1(k,G_j)}{n^i{}_1(k,G_j) + n^i{}_0(k,G_j)} \tag{1}$$

in which $n_1{}^i(k,G_j)$ is the number of liquefied meshes, while $n_0{}^i(k,G_j)$ is the number of unliquefied meshes.

Formulation for liquefaction hazard mapping

Since the historic earthquakes are different in its magnitude and epicenter, the most appropriate liquefaction hazard graph for the assumed regional area can be expressed in the following equation:

$$P[L \mid k,G_j] = \sum_i w^i\, P\left[L^i \mid k,G_j\right] \tag{2}$$

where w^i is weighing coefficient to evaluate the contribution for the liquefaction hazard graph of the i-th earthquake.

Actually there are few records of liquefaction for the contribution for the past earthquakes more than 100 years ago, while in the recent earthquakes we could collect many data of liquefaction sites and their hazard situations. In order to comply such situations, the following weighing coefficient is introduced:

$$w_D^i = \frac{\sum_k n^i{}_1(k,G_j)}{\sum_i \sum_k \left\{n^i{}_1(k,G_j) + n^i{}_0(k,G_j)\right\}} \tag{3}$$

in which the recent earthquake having many liquefaction hazard data is greatly evaluated more than old earthquakes with insufficient hazard data.

In order to predict the future seismic hazard of liquefaction for the assumed regional area, the probabilistic approach is adopted to make the quantitative estimate of the liquefaction hazard at each site for a given earthquake. The probability of liquefaction $P[L \mid x]$ at the site (x) can be expressed by:

$$P[L \mid x] = \sum_i P_{EQ}\left[L^i \mid x\right] P[EQ_i] \tag{4}$$

in which $P[EQ_i]$ is the probability that the earthquake EQ_i occurs and the conditional probability of liquefaction $P_{EQ}[L_i \mid x]$, given that event EQ_i occurs, is expressed by:

$$\begin{aligned} P_{EQ}\left[L^i \mid x\right] &= \sum_\nu P\left[L^i \mid k_\nu, G(x)\right] P\left[k_\nu \mid G(x), EQ_i\right] \\ &= \sum_\nu P\left[L^i \mid k_\nu, G(x)\right] \cdot \\ &\qquad \int P\left[k_\nu \mid s\right] f_{S_\nu}\left[s(x) \mid EQ_i\right] ds \end{aligned} \tag{5}$$

where k_ν is the ν-th seismic intensity shown in Fig.2, and G(x) is the geological characteristics of the site (x), and $f_{S_V}[s(x)]$ is the probability of the response velocity S_V of the ground surface.

CASE STUDY

Numerical study was conducted for Kanto district in Fig.3 including Tokyo metropolitan area in which historically many earthquakes occured not only at the fringe of the Pacific Ocean but also at the inland of Kanto plain. Several hundreds of liquefaction sites in this district are furnished in the digital database which are designed to be compatible to the GIS database. Table 2 shows nine historic earthquakes which are selected in this analysis. Recent earthquakes such as 1923 Kanto, 1931 Nishi-saitama and 1987 Chibaken--toho-oki events shown in this Table have sufficient and reliable records of liquefaction sites, while older earthquakes have limited records less than 100.

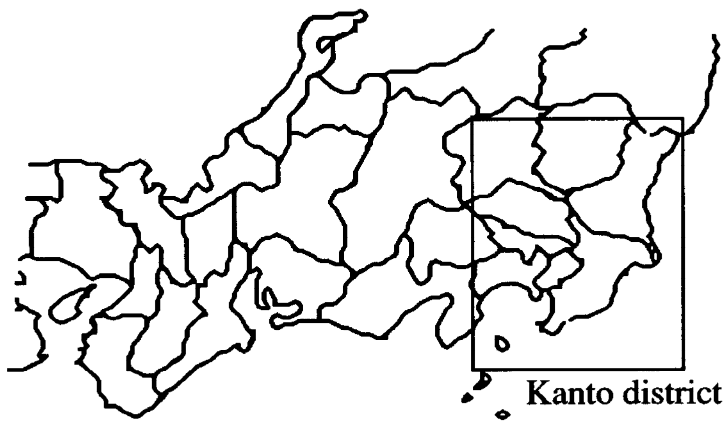

Fig.3 Regional area adopted for the case study.

Table 2. Historic earthquakes in which the location data of liquefaction are available (Utsu, 1982).

No.	Earthquake	Year	Magnitude	Records
1	Genroku	1703	8.2	7
2	Ansei-toukai	1854	8.4	85
3	Ansei-nankai	1854	8.4	85
4	Edo	1855	6.9	13
5	Tokyo-wan	1894	7.0	32
6	Kasumiga-ura	1895	7.2	16
7	Kanto	1923	7.9	705
8	Nishi-saitama	1931	6.9	119
9	Chibaken-toho-oki	1987	6.7	255

Fig.4 reveals the relation between the liquefaction hazard and the geological code (geomorphological land classification code) for those nine historic earthquakes. The ordinate of these graphs is the probability of liquefaction defined by the following equation:

$$P\left[L^i \mid k_n, G_j\right] = \sum_{\nu=1}^{n} P\left[L^i \mid k_\nu, G_j\right] \tag{6}$$

And the abscissa shows the geological code given in Table 1.

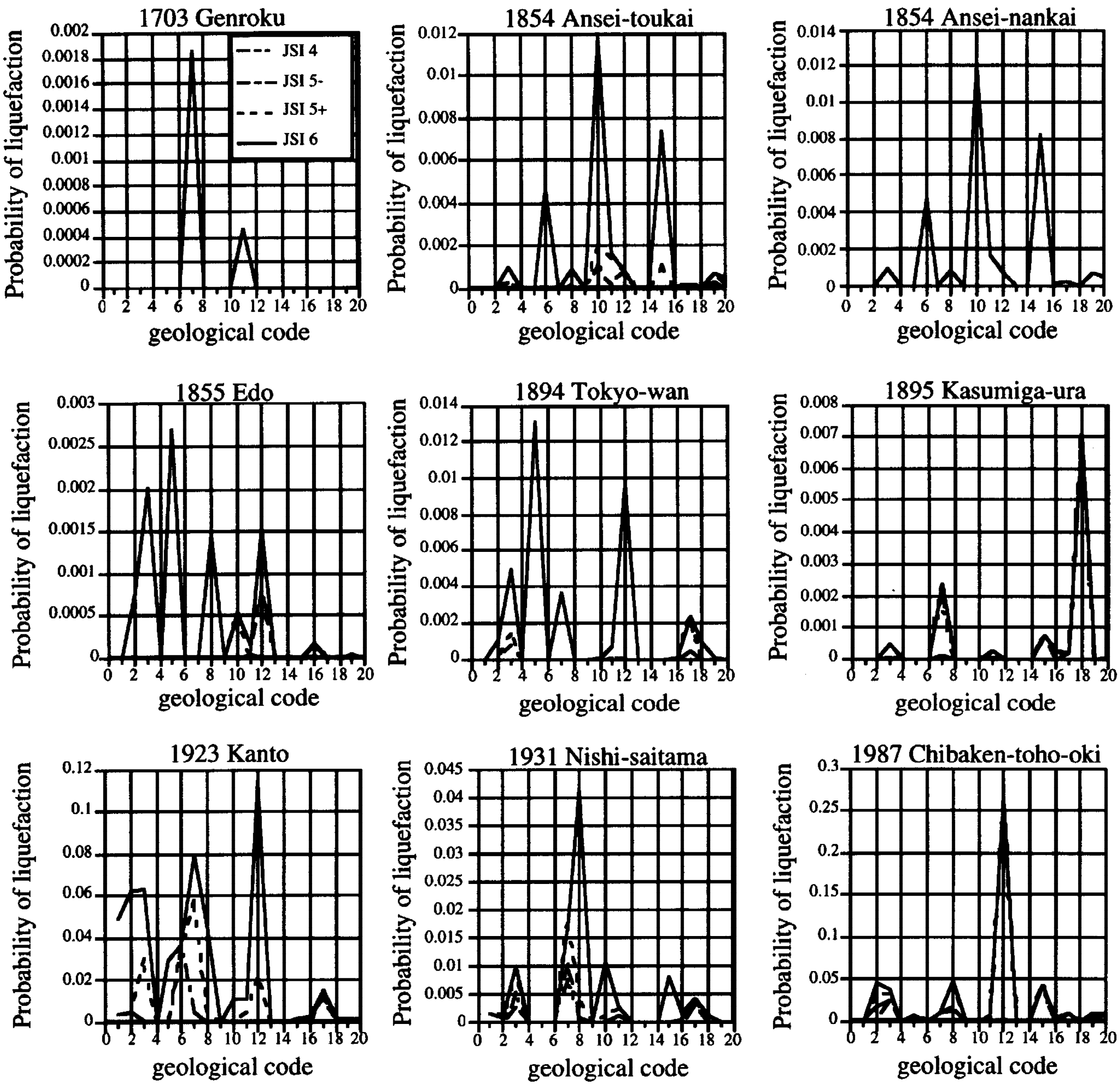

Fig.4 Relation between the liquefaction hazard and geological code (geomorphological land classification code) in the regional area of Kanto district.

Fig.4 shows that the reclaimed land (code 12) is remarkably liquefaction-sensitive in the 1923 Kanto and 1987 Chibaken-toho-oki earthquakes, the alluvial fan (code 10) is typical in the 1854 Ansei-tokai and -nankai earthquakes, and the delta (code 5) shows high probability of liquefaction in 1855 Edo and 1894 Tokyo-wan earthquakes, while the natural levee (code 7,8,18) is sensitive in 1703 Genroku, 1895 Kasumiga-ura and 1934 Nishi-saitama earthquakes in which the liquefaction sites are concentrated at the riverside of the Tone and the Edo Rivers. These different topographical characteristics of Fig.4 are caused by the varieties of magnitude and epicentral location of each earthquake, so that the liquefaction hazard graph for Kanto district must be integrated with all these graphs.

Fig.5 shows the average liquefaction hazard graph $P[L_D \mid k_n, G_j]$ for each geomorphological land classification of Kanto district. The profile of this figure mainly reflects the characteristics of the 1987 Chibaken-toho-oki and 1923 Kanto earthquakes because of their many location data of liquefaction points. Four lines in Fig.5 means the probability of liquefaction for each seismic intensity (JSI).

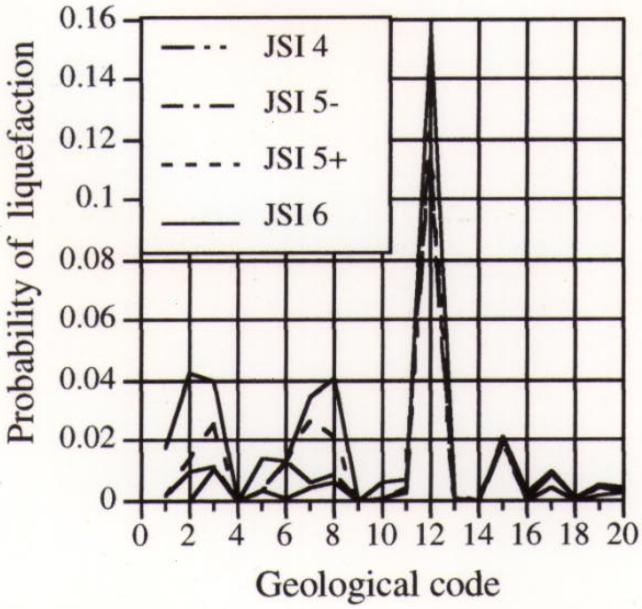

Fig.5 Average liquefaction hazard graph for the regional area.

Photo 1 displays the epicentral map of historical earthquakes occuring in Kanto district, the magnitude of which is greater than 6, and also this photo indicates the map of liquefactions in the 1987 Chibaken-toho-oki earthquake, where the liquefaction points are reported in the reclaimed land of Tokyo Bay area, the riverside of the Tone River and highly seismic intensity area facing the Pacific Ocean.

Photo 2 classifies each mesh into the geomorphological land based on Table 1. According to this photo, the reclaimed area surrounds the Tokyo Bay and the alluvial delta extends along two big rivers Tone and Edo.

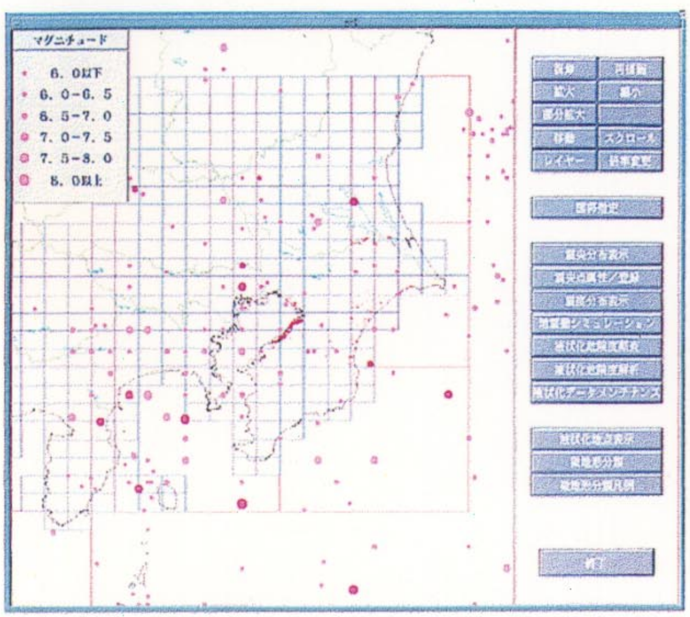

Photo 1. Epicentral map and liquefaction sites of the 1987 Chibaken-toho-oki earthquake.

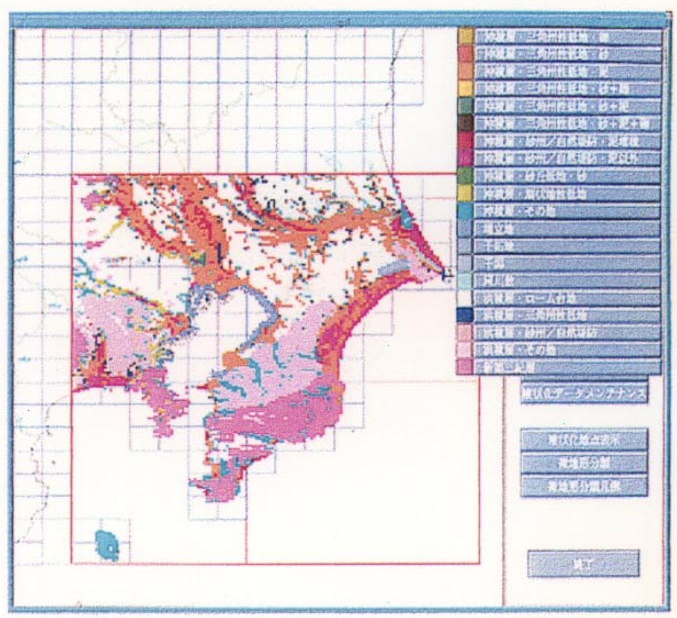

Photo 2. Geomorphological land classification map of the regional area.